Stem Cell Reports
Article

OPEN ACCESS

Elevated Oxidative Stress Impairs Hematopoietic Progenitor Function in C57BL/6 Substrains

Antonio Morales-Hernández,[1] Alice Martinat,[1] Ashley Chabot,[1] Guolian Kang,[2] and Shannon McKinney-Freeman[1,*]

[1]Department of Hematology, St. Jude Children's Research Hospital, Memphis, TN 38105, USA
[2]Department of Biostatistics, St. Jude Children's Research Hospital, Memphis, TN 38105, USA
*Correspondence: shannon.mckinney-freeman@stjude.org
https://doi.org/10.1016/j.stemcr.2018.06.011

SUMMARY

C57BL/6N (N) and C57BL/6J (J) mice possess key genetic differences, including a deletion in the *Nicotinamide nucleotide transhydrogenase* (*Nnt*) gene that results in a non-functional protein in J mice. NNT regulates mitochondrial oxidative stress. Although elevated oxidative stress can compromise hematopoietic stem and progenitor cell (HSPC) function, it is unknown whether N- and J-HSPCs are functionally equivalent. Here, we report that J-HSPCs display compromised short-term hematopoietic repopulating activity relative to N-HSPCs that is defined by a delay in lymphoid reconstitution and impaired function of specific multi-potent progenitor populations post transplant. J-HSPCs also displayed elevated reactive oxygen species (ROS) relative to N-HSPCs post transplant and upregulate ROS levels more in response to hematopoietic stress. *Nnt* knockdown in N-HSPCs recapitulated J-HSPCs' short-term repopulating defect, indicating that NNT loss contributes to this defect. In summary, C57BL/6N and C57BL/6J HSPCs are not functionally equivalent, which should be considered when determining the substrain most appropriate for investigations of HSPC biology.

INTRODUCTION

Inbred mice play a major role in biomedical research by allowing researchers to perform reproducible experiments in a uniform genetic background. The C57BL/6 mouse strain is currently one of the most commonly used inbred mouse strains. In 1948 the C57BL/6J mouse (J mice) strain was established at the Jackson Laboratory. In 1951 the National Institutes of Health established a J-mouse colony designated "C57BL/6N" (N mice). In 1974 the Charles Rivers Laboratory began to its own C57BL/6N colony, which was called "C57BL/6NCrl" (referred to here as N mice). J mice and N mice, which are now separated by approximately 200 generations, display phenotypic differences (Clapcote and Roder, 2004; Grottick et al., 2005; Mayorga and Lucki, 2001; Mekada et al., 2009; Radulovic et al., 1998; Siegmund et al., 2005; Stiedl et al., 1999) in glucose metabolism (Freeman et al., 2006; Huang et al., 2006; Toye et al., 2005), alcohol metabolism (Green et al., 2007; Khisti et al., 2006), and drug (anesthetic, tumorigenic) sensitivity (Diwan and Blackman, 1980; Roth et al., 2002). Whole-genome comparisons of N and J mice have revealed 34 coding SNPs, two coding insertion/deletions (indels), 146 non-coding SNPs, 54 non-coding indels, and 43 structural variants (Simon et al., 2013). Importantly, J mice also possess a five-exon deletion in the *Nicotinamide nucleotide transhydrogenase* (*Nnt*) gene (Huang et al., 2006). In mammalian cells, NNT is integral to the inner mitochondrial membrane where it catalyzes the reversible transfer of hydrogen between NAD^+ and $NADP^+$. Consequently, J mice display significantly impaired mitochondrial function (Ronchi et al., 2013). NNT also regulates mitochondrial redox via the glutathione and thioredoxin/peroxiredoxin pathways (Hoek and Rydström, 1988). J mice have differential sensitivity to genetic deletion of antioxidant proteins, which is believed to be a direct result of the loss of *Nnt* (Huang et al., 2006, 2010). Knockout mice for genes like *Sod2* generated on a J background display tissue damage even under homeostatic conditions (Huang et al., 2006, 2010). However, despite these known phenotypic and genotypic differences, about 58% of published studies using C57BL/6 mice do not fully describe their genetic background (Fontaine and Davis, 2016).

C57BL/6 mice are heavily used in the study of hematopoietic stem cells (HSCs) and transplantation because of the convenience of the CD45 congenic system to track hematopoietic repopulating activity. HSCs can reconstitute the entire hematopoietic system after transplantation into hosts whose own hematopoietic compartment has been ablated. One of the most harmful phenomena occurring during HSC transplantation (HSCT) is the increase in both intracellular and extracellular reactive oxygen species (ROS) (Mantel et al., 2015). ROS are by-products of oxidative phosphorylation for energy production. Cellular antioxidants function continuously to control ROS levels, thereby regulating the proliferation, growth, signal transduction, and gene expression of the cells (Chen et al., 2008, 2009; Ergen and Goodell, 2010; Lewandowski et al., 2010). Nevertheless, when ROS levels increase dramatically or the antioxidant capacity of cells is compromised, ROS stress occurs. During transplantation, HSCs are

sequentially exposed to dramatically different oxygen environments: hypoxia (in bone marrow [BM]), relatively low oxygen when recruited to the circulation during mobilization, normoxia (after collection or during *in vitro* culture), relatively low oxygen again after intravenous reinfusion, and finally hypoxia (after homing back to the BM) (Hao et al., 2011). Elevated ROS levels are well known to compromise HSC lifespan (Ito et al., 2006), self-renewal (Ito et al., 2004; Le et al., 2016), and differentiation (Cao et al., 2016; Maryanovich et al., 2015). However, despite the known sensitivities of HSCs and their downstream progenitors to ROS levels, it has never been reported whether hematopoietic stem and progenitor cells (HSPCs) isolated from J and N mice are functionally equivalent.

Thus, here we examined the frequency and function of HSPCs isolated from N and J mice. We discovered that N-HSPCs display superior short-term repopulating activity relative to J-HSPCs and that J-HSPCs are much more sensitive to oxidative stress. Also, *Nnt* knockdown in N-HSPCs recapitulates the functional defects seen in J-HSPCs. These findings highlight the necessity for intense scrutiny when determining the appropriate genetic background in studies involving HSPCs, especially those involving HSCT. Furthermore, our findings emphasize the importance of proper reporting of genetic background in peer-reviewed articles.

RESULTS

C57BL/6N and C57BL/6J Mice Display Similar Frequencies of Peripheral Blood and Bone Marrow Hematopoietic Populations

We first examined whether there were any overt differences in the distribution of the mature blood lineages in N and J mice. No differences were seen in either absolute blood counts or the relative frequencies of peripheral blood (PB) B cells, T cells, or myeloid cells in 8- to 10-week-old N and J mice (Figure S1A). We also examined N- and J-mouse BM for the absolute frequency of HSPCs. We saw no differences in the relative frequency of long-term HSCs (LT-HSC; $Lin^-SCA1^+CKIT^+FLT3^-CD48^-CD150^+$), short-term HSCs (ST-HSC; $Lin^-SCA1^+CKIT^+FLT3^-CD48^-CD150^-$), multipotent progenitors (MPP2: $Lin^-SCA1^+CKIT^+FLT3^-CD48^+CD150^+$; MPP3: $Lin\text{-}SCA1^+CKIT^+FLT3^-CD48^+CD150^-$; MPP4: $Lin\text{-}SCA1^+CKIT^+FLT3^+CD48^+CD150^-$), common myeloid progenitors (CMP; $Lin^-SCA1^-CKIT^+CD34^+CD16/32^{med}$), granulocyte-macrophage progenitors (GMP; $Lin^-SCA1^-CKIT^+CD34^+CD16/32^{high}$), megakaryocyte-erythroid progenitors (MEP; $Lin^-SCA1^-CKIT^+CD34^-CD16/32^-$), or common lymphoid progenitors (CLP; $Lin^-SCA1^{med}CKIT^{med}CD127^+$) in these mice (Figure S1B). To grossly examine their function, we isolated BM $Lineage^-SCA\text{-}1^+CKIT^+$ (LSK) cells from N and J mice and tested them for colony-forming unit (CFU) potential in semi-solid media supplemented with hematopoiesis-promoting cytokines. We observed no differences in the absolute number or types of CFUs yielded by N- and J-LSK cells (Figure S1C).

J-HSPCs Display Compromised Short-Term *In Vivo* Repopulating Activity

We next examined the *in vivo* repopulating potential of N- and J-HSPCs. Here, LSK cells isolated from 8- to 10-week-old N or J mice ($CD45.2^+$) were transplanted along with an equal number of competitor LSK cells ($CD45.1^+$) into lethally irradiated recipients (CD45.1/$CD45.2^+$) (Figure 1A). For 12 weeks post transplant, N-HSPCs displayed significantly increased repopulation of recipient PB relative to J-HSPCs (Figure 1B). This advantage was transient, no longer significant at 16 and 20 weeks post transplant, and appeared primarily driven by enhanced reconstitution of the B and T cell lineages (Figure 1C). BM from primary recipients was next transplanted into secondary recipients (Figure S2A). In secondary recipients, J-BM cells also displayed a short-term repopulating defect relative to N-BM cells (Figure S2B). Examination of the major BM compartments (BMC) of primary recipients revealed significantly enhanced reconstitution of donor-derived CLPs of N recipients relative to J recipients at 4 and 8 weeks post transplant (Figure 1D). This enhanced chimerism was absent by 12 weeks post transplant (Figure 1D), which is consistent with the short-term repopulating advantage seen in the lymphoid PB lineages of these recipients.

We next quantified the frequency of long-term competitive repopulating units (CRUs) in J and N mice via limiting dilution transplant. J- or N-BM ($CD45.2^+$) was transplanted at limiting dilution along with a 200,000 competitive BM cells ($CD45.1^+$) into lethally irradiated recipient mice ($CD45.1/CD45.2^+$) (Figure 2A). Again, J-BM displayed a transient repopulating defect relative to N-BM (Figure 2B). We next applied Poisson statistics to calculate the number of repopulating units in each substrain. There was no significant difference in the frequency of CRUs in J- and N-BM (Figure 2C), confirming that the repopulating defect in the J-HSPCs is restricted to short-term progenitors.

J-HSPC Short-Term Repopulating Defect Results from Perturbed Function of MPP3 and MPP4 Cells Post Transplant

LSK cells comprise multiple HSPC populations that display distinct repopulation kinetics and lineage potential post transplant (Pietras et al., 2015; Yilmaz et al., 2006) (Figure 3A). Thus, to better define the short-term

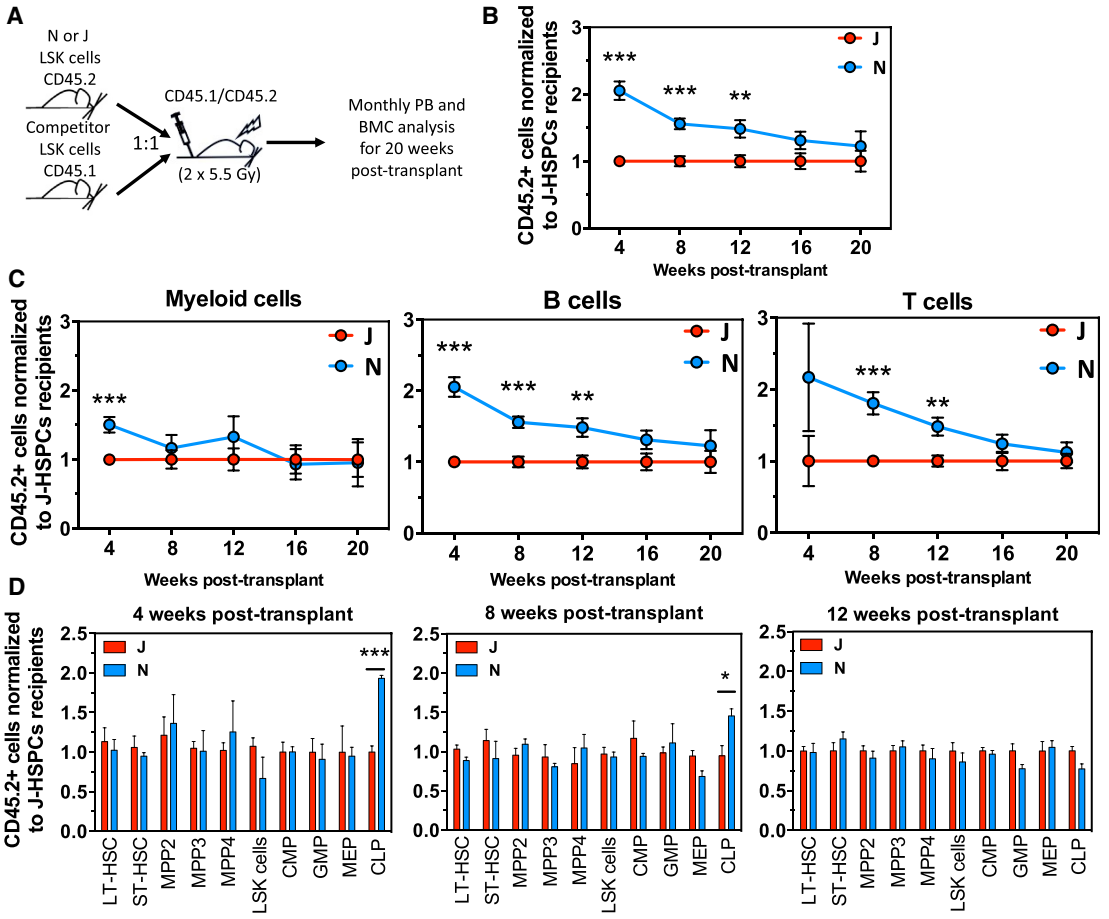

Figure 1. J-HSPCs Display a Short-Term Repopulating Defect

(A) N- or J-LSK cells (CD45.2) were mixed 1:1 with competitor LSK cells (CD45.1) and injected into lethally irradiated recipient mice (CD45.1/CD45.2). $CD45.2^+$ chimerism of the PB was examined by flow cytometry every 4 weeks for 20 weeks post transplant.

(B) Normalized $CD45.2^+$ chimerism in total recipient PB after transplant.

(C) Normalized $CD45.2^+$ chimerism among the myeloid ($GR1^+CD11B^+$) and lymphoid (B cells as $B220^+$ and T cells as $CD4^+CD8^+$) lineages in the recipient PB post transplant.

(D) Normalized $CD45.2^+$ chimerism among the BMC at 4, 8, and 12 weeks post transplant. Data presented are normalized to the $CD45.2^+$ chimerism observed in recipients of J-LSK cells.

Data from three independent transplants are presented as mean ± SEM. Donor mice, $n \geq 3$ pooled per transplant. Recipient mice, $n \geq 5$ per transplant. *$p < 0.05$, **$p < 0.005$, ***$p < 0.001$, significantly different from recipients of J-LSK cells.

repopulating defect of J-LSK cells, we next examined the repopulating activity of LT-HSC, ST-HSC, MPP2, MPP3, and MPP4 cells isolated from N and J mice. Each population was isolated from N- and J-mouse BM (CD45.2) and transplanted into sublethally irradiated recipients ($CD45.1/CD45.2^+$) (Figure 3B). J- and N-HSPC subpopulations displayed similar lineage output post -transplant (Figure 4). However, N-MPP3 and N-MPP4 cells displayed superior repopulating activity relative to J-MPP3 and J-MPP4 cells as early as 10–15 days post transplant (Figure 3C). An examination of the BM of transplant recipients revealed that N-MPP3 and N-MPP4 cells repopulated the CLP compartment more robustly than J-MPP3 and J-MPP4 cells 1 month post transplant (Figure S3). MPP3 and MPP4 cells reconstitute lymphoid populations in the PB before other HSPC compartments (Figure 4) (Pietras et al., 2015). The failure to robustly repopulate the CLP compartment at early time points post transplant likely contributes to the short-term PB repopulating defect of J-HSPCs relative to N-HSPCs. Furthermore, the overall output of J-MPP3 and J-MPP4 cells is similar post transplant, while N-MPP3 cells contribute more robustly to both the PB and BMC than N-MPP4 cells (Figures 3C and S3). Thus, the relative behavior of these HSPC subsets is different after transplant between these strains of mice.

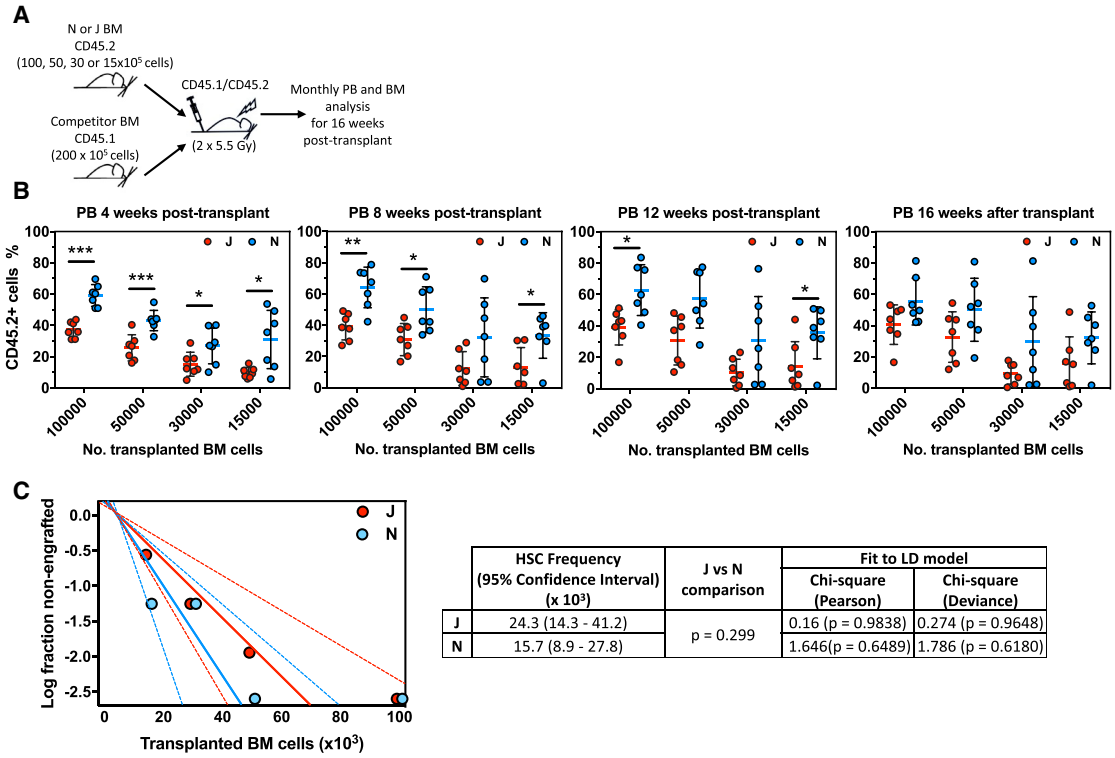

	HSC Frequency (95% Confidence Interval) (x 10^3)	J vs N comparison	Fit to LD model	
			Chi-square (Pearson)	Chi-square (Deviance)
J	24.3 (14.3 - 41.2)	p = 0.299	0.16 (p = 0.9838)	0.274 (p = 0.9648)
N	15.7 (8.9 - 27.8)		1.646(p = 0.6489)	1.786 (p = 0.6180)

Figure 2. J and N Mice Have Similar Numbers of Long-Term Functional Repopulating Units

(A) Decreasing numbers of N- or J-BM cells (CD45.2) were mixed with 200,000 competitor BM cells (CD45.1) and injected into lethally irradiated recipient mice (CD45.1/CD45.2). $CD45.2^+$ chimerism of the PB was examined by flow cytometry every 4 weeks for 16 weeks post transplant.

(B) $CD45.2^+$ chimerism in total recipient PB after transplant.

(C) At 16 weeks post transplant, recipients were scored as non-engrafted or engrafted (i.e., $CD45.2^+$ PB chimerism >1% in the T cell, B cell, and myeloid cell lineages) and the frequency of HSC (i.e., CRUs) calculated via Poisson statistics. χ^2 analysis revealed a good fit to the limiting dilution model.

Data are presented as mean ± SEM. Donor mice, $n \geq 3$ pooled per transplant. Recipient mice, $n \geq 7$ per transplant.*$p < 0.05$, **$p < 0.005$, ***$p < 0.001$, significantly different from recipients of J-BM cells.

J-HSPCs Display Higher Levels of Oxidative Stress than N-HSPCs Post Transplant and in Response to pI:pC Injection

As the *Nnt* gene is non-functional in C57BL/6J mice, and NNT is well known to regulate oxidative stress (Hoek and Rydström, 1988), we next examined ROS levels in the BM of mice transplanted with N- or J-LSK cells. For these experiments, J- and N-LSK cells were transplanted competitively as depicted in Figure 1A and recipient $CD45.2^+$ BMCs analyzed at 4, 8, 12, and 20 weeks post transplant for ROS levels using the ROS reporter CellROX Deep Red (Lin et al., 2012; Strohecker et al., 2015). ROS levels were significantly higher in the donor-derived CLP compartment of mice transplanted with J-LSK cells relative to N-LSK cell recipients up to 12 weeks post transplant (Figure 5). J-derived ST-HSC also displayed elevated ROS at 4 and 8 weeks post transplant (Figure 5). These data suggest that N-ST-HSCs and CLPs cope with transplant-induced oxidative stress better than J-ST-HSCs and CLPs, and are consistent with a short-term repopulating defect driven primarily by a loss of lymphoid repopulation.

To further explore the sensitivity of J- and N-HSPCs to oxidative stress, we next examined the response of J- and N-BM HSPCs to ROS induction via treatment with polyinosinic:polycytidylic acid (pI:pC). pI:pC mimics viral infection by inducing a type I interferon response, which causes an increase of ROS in HSCs (Walter et al., 2015). The BMC of N and J mice injected with pI:pC were examined 24 hr post injection (Figure 6A). N and J mice both responded to pI:pC injection by increasing BMC numbers and ROS levels in all BMC examined relative to controls (Figures 6B and S4). However, the magnitude of ROS increase was significantly greater in J mice than in N mice in all compartments

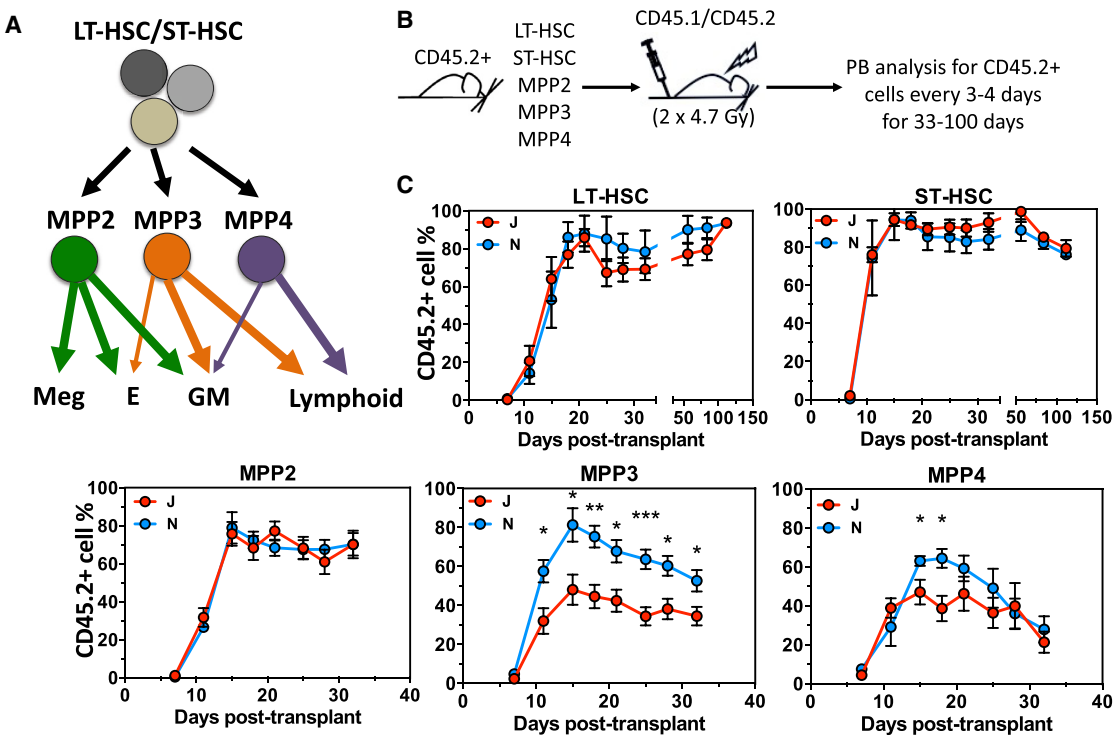

Figure 3. J-MMP3 and J-MPP4 Display a Repopulating Defect Relative to N-MPP3 and N-MPP4

(A) Schematic representation of the multipotent progenitor hierarchy and their relative contribution to the PB lineages (adapted from Pietras et al., 2015).

(B) CD45.2 N or J-HSPCs (LT-HSC, ST-HSC, MPP2, MPP3, and MPP4) were transplanted into sublethally irradiated recipients (CD45.1/CD45.2). Recipient PB was examined for CD45.2$^+$ cells and myeloid (GR1$^+$CD11B$^+$) and lymphoid (B cells as B220$^+$ and T cells as CD4$^+$CD8$^+$) cells by flow cytometry every 3–4 days for 33–100 days.

(C) Chimerism percentage in the recipient mice PB after transplant.

Data from two independent transplants are presented as mean ± SEM. Donor mice, n = 3 pooled per transplant. Recipient mice, n = 5 per transplant. *p < 0.05, **p < 0.005, ***p < 0.001, significantly different from recipients of J-HSPCs.

examined except committed myeloid progenitors (i.e., CMP, GMP, and MEP) (Figure 6B).

HSPCs from N and J mice treated and not treated with pI:pC were also assayed for CFU potential. We observed a significant decrease in both the number and size of CFUs produced by J-HSPC pI:pC-treated mice (Figures 6C and 6D). J-HSPCs isolated from pI:pC-treated mice also yielded fewer mixed-lineage colonies (e.g., CFU-GEMM and CFU-GM) (Figure 6E). Similarly, BM from N and J mice treated or untreated with pI:pC was tested for pre-B-CFU potential (Figures 6F and 6G). Although we did not detect any differences in absolute numbers of pre-B-CFUs from N and J cells, we did observe a mild decrease in the size of the colonies generated by J-HSPCs after pI:pC treatment, relative to N-HSPCs (Figures 6F and 6G). These changes were all exacerbated by the addition of $ZnCl_2$, which further increases oxidative stress (Kinazaki et al., 2011; Wiseman et al., 2010). In sum, J-HSPCs display increased sensitivity to induced oxidative stress relative to N-HSPCs, which disparately affects their self-renewal and differentiation potential, as reflected by CFU numbers, type, and colony size.

Nnt Loss Contributes to the Repopulating Defect of J-HSPCs

One major genetic difference between J and N mice is the disruption of the *Nnt* gene (Huang et al., 2006). In N-HSPCs, *Nnt* expression is largely restricted to MPP subsets rather than HSCs, consistent with our previous observations (Figure S5A). To determine whether loss of *Nnt* contributes to the J-HSPC phenotype, we next tested whether *Nnt* knockdown in N-HSPCs recapitulates the PB repopulating defect of J-HSPCs. To this end, J- and N-LSK cells isolated from 8- to 10-week-old mice (CD45.2$^+$) were transduced with lentiviral control or *Nnt* short hairpin RNAs (*Nnt*-shRNAs). Transduced cells (i.e., mCherry$^+$) were then sorted and transplanted along with an equal number of competitor mock-transduced LSK cells (CD45.1$^+$) into lethally irradiated recipients (CD45.1/CD45.2$^+$) (Figures

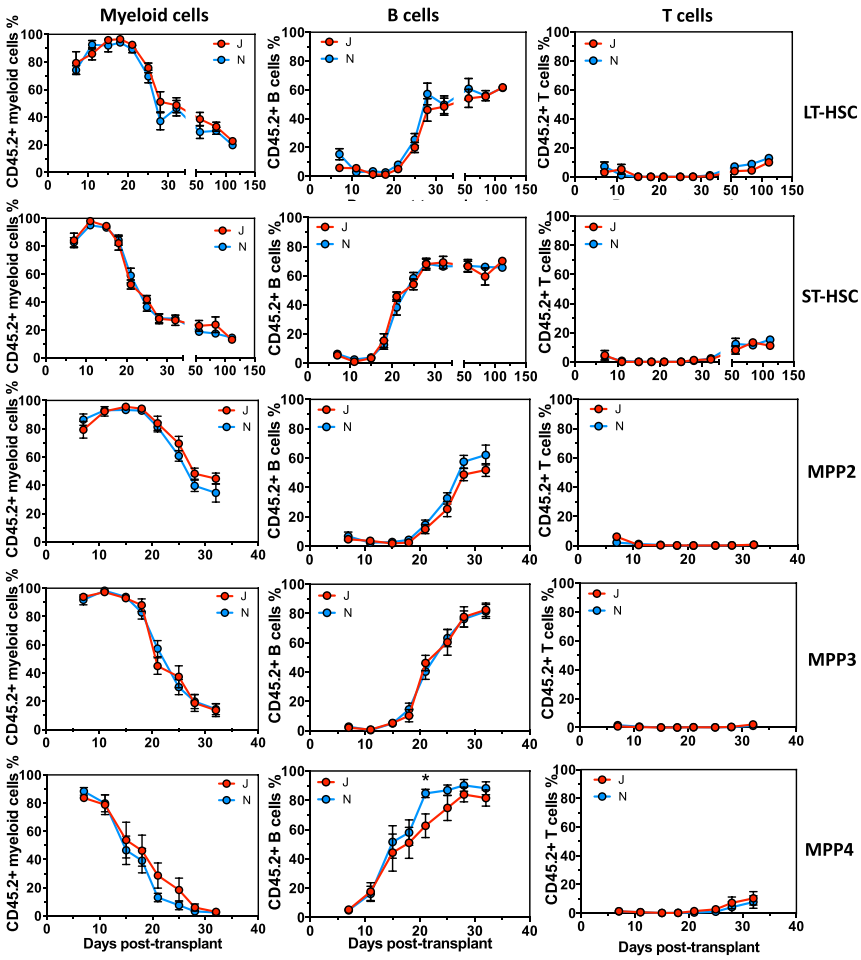

Figure 4. J- and N-HSPC Subpopulations Display Similar Lineage Output Post Transplant

HSPC subpopulations (LT-HSC, ST-HSC, MPP2, MPP3, and MPP4) from J or N mice (CD45.2) were transplanted into sublethally irradiated recipients (CD45.1/CD45.2). Recipient PB was examined for CD45.2$^+$ cells and myeloid (GR1$^+$CD11b$^+$) and lymphoid (B cells as B220$^+$ and T cells as CD4$^+$CD8$^+$) cells by flow cytometry every 3–4 days for 33–100 days. Percentage of myeloid, B, and T cells among the CD45.2$^+$ cells produced by HSPC subpopulations post transplant. Data from two independent transplants are presented as mean ± SEM. Donor mice, n = 3 pooled per transplant. Recipient mice, n = 5 per transplant. *p < 0.05, significantly different to recipients of J-HSPCs.

7A and 7B). Knockdown of *Nnt* in N-HSPCs yielded a short-term PB repopulating defect that mirrored that of J-HSPCs (Figure 7C). As expected, treatment of J-HSPCs with *Nnt*-shRNAs had no effect on their repopulating activity, confirming the specificity of *Nnt*-shRNAs (Figure 7D). *Nnt* knockdown in N-HSPCs also recapitulated the short-term CLP repopulating defect (Figure S5B) and the increased ROS levels (Figure S5C) of J-HSPCs. Thus, the absence of a functional *Nnt* gene in J-HSPCs very likely contributes directly to their short-term repopulating defect and hypersensitivity to stress-induced ROS.

DISCUSSION

Here, we compared the hematopoietic system of two commonly used C57BL/6 mice substrains (J and N). One major genetic difference between these substrains is the disruption of the *Nnt* gene in J mice (Huang et al., 2006), which encodes one of the main enzymes controlling oxidative stress (Hoek and Rydström, 1988). HSPCs experience severe oxidative stress during HSCT (Mantel et al., 2015). Our results reveal that J-HSPCs have a significant disadvantage in short-term PB repopulating activity after transplant relative to N-HSPCs. This disadvantage is most acute in the lymphoid lineages (B and T cells) and coincides with a reduced ability to reconstitute the CLP compartment post transplant. We further determined that this repopulating defect results specifically from the compromised function of J-MPP3 and J-MPP4 cells post transplant. MPP3 and MPP4 cells are responsible for the short-term reconstitution of lymphoid lineages at acute time points post transplant. Indeed, J-HSPCs, particularly J-CLPs, displayed higher levels of ROS both post transplant and in response to oxidative stress. Finally, we show that knockdown of *Nnt* in N-HSPCs recapitulates the repopulating defect of J-HSPCs after transplantation, strongly suggesting that *Nnt* loss is a major contributor to the functional differences of J- and N-HSPCs during HSCT.

The absolute output of discrete HSPC compartments relative to each other post transplant has been described (Pietras et al., 2015). In our comparison of C57BL/6J and

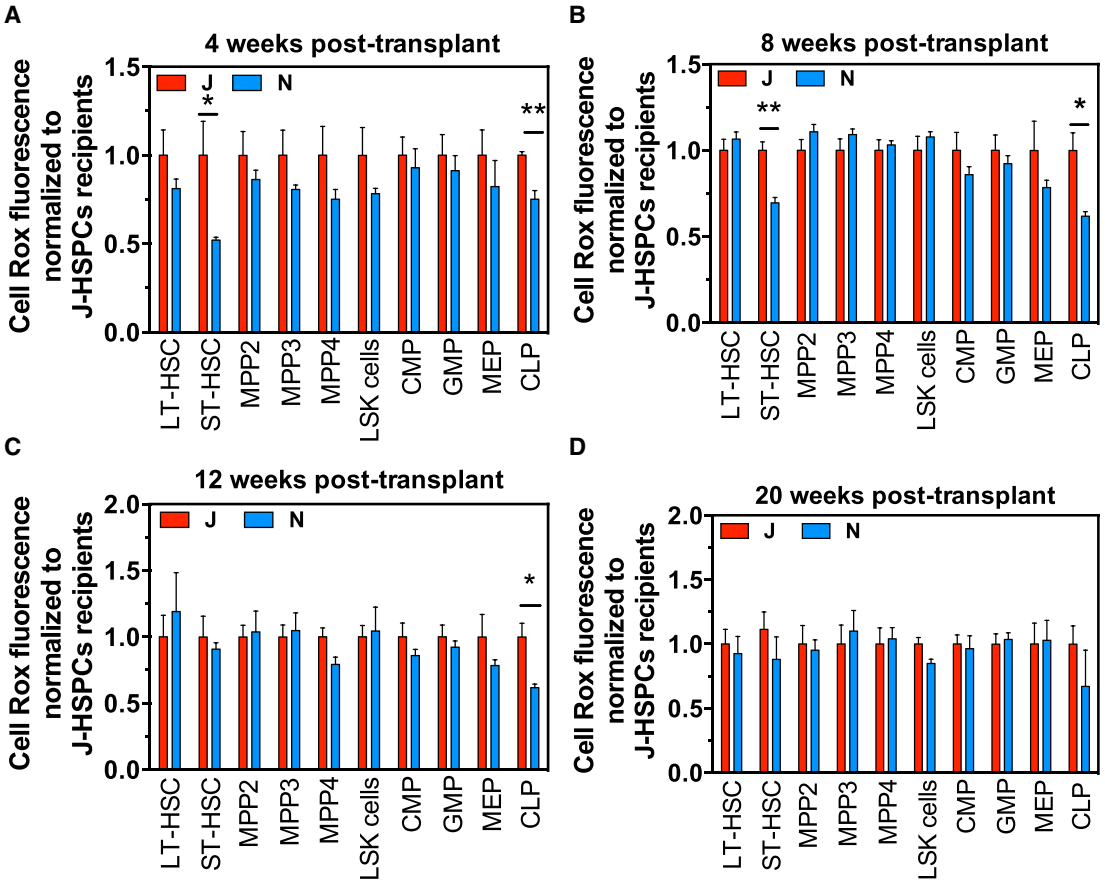

Figure 5. BMC Derived from Transplanted J-HSPCs Display Elevated ROS Levels Post Transplant

N- or J-LSK cells (CD45.2) were mixed 1:1 with competitor LSK cells (CD45.1) and injected into lethally irradiated recipients (CD45.1/CD45.2). Normalized CellROX fluorescence in CD45.2$^+$ cells in each BMC after 4 (A), 8 (B), 12 (C), and 20 (D) weeks after transplant. Data presented are normalized to the fluorescence levels in J mice. Data from two independent transplants are presented as mean ± SEM. Donor mice, n ≥ 3 pooled per transplant. Recipient mice, n ≥ 4 per time point. *p < 0.05, **p < 0.005, significantly different from recipients of J-LSK cells.

C57BL/6N substrains, we noted differences in the absolute output of distinct HSPC compartments between J and N mice. Specifically, while J-MPP3 and J-MPP4 cells were similar in their absolute contribution to the PB post transplant, N-MPP3 cells contributed significantly more cells to the PB than N-MPP4 cells after transplantation. Furthermore, both N-MPP3 and N-MPP4 cells contributed more to PB and BM populations than J-MPP3 and J-MPP4 cells. Thus, the behavior of MPP3 and MPP4 cells relative to each other post transplant differs between C57BL/6 substrains. These differences could skew results and conclusions depending on which substrain is utilized for a particular set of experiments.

Murine HSPCs with low ROS levels are more quiescent and exhibit an increased self-renewal potential compared with HSPCs with higher ROS levels (Testa et al., 2016). Our results reveal that some J-HSPC-derived BMC contain higher ROS levels acutely post transplant than BMC reconstituted by N-HSPCs. This finding suggests that J-HSPCs manage oxidative stress levels poorly relative to N-HSPCs during transplantation. This elevated ROS likely contributes to the short-term repopulating defect of J-HSPCs. Furthermore, ROS induction via treatment with pI:pC injections revealed that J-HSPCs fail to resolve elevated oxidative stress as efficiently as N-HSPCs, which was detrimental to their self-renewal and differentiation potential. It is also important to emphasize that unlike the functional differences apparent after transplant, no difference in the frequency of any BMC or PB lineage between these two substrains was observed at steady state. This reinforces the idea of stress during transplantation as the cause of the repopulating defect in J-HSPCs.

We propose that the lack of the *Nnt* gene in J-HSPCs specifically diminished their *in vivo* repopulating activity due

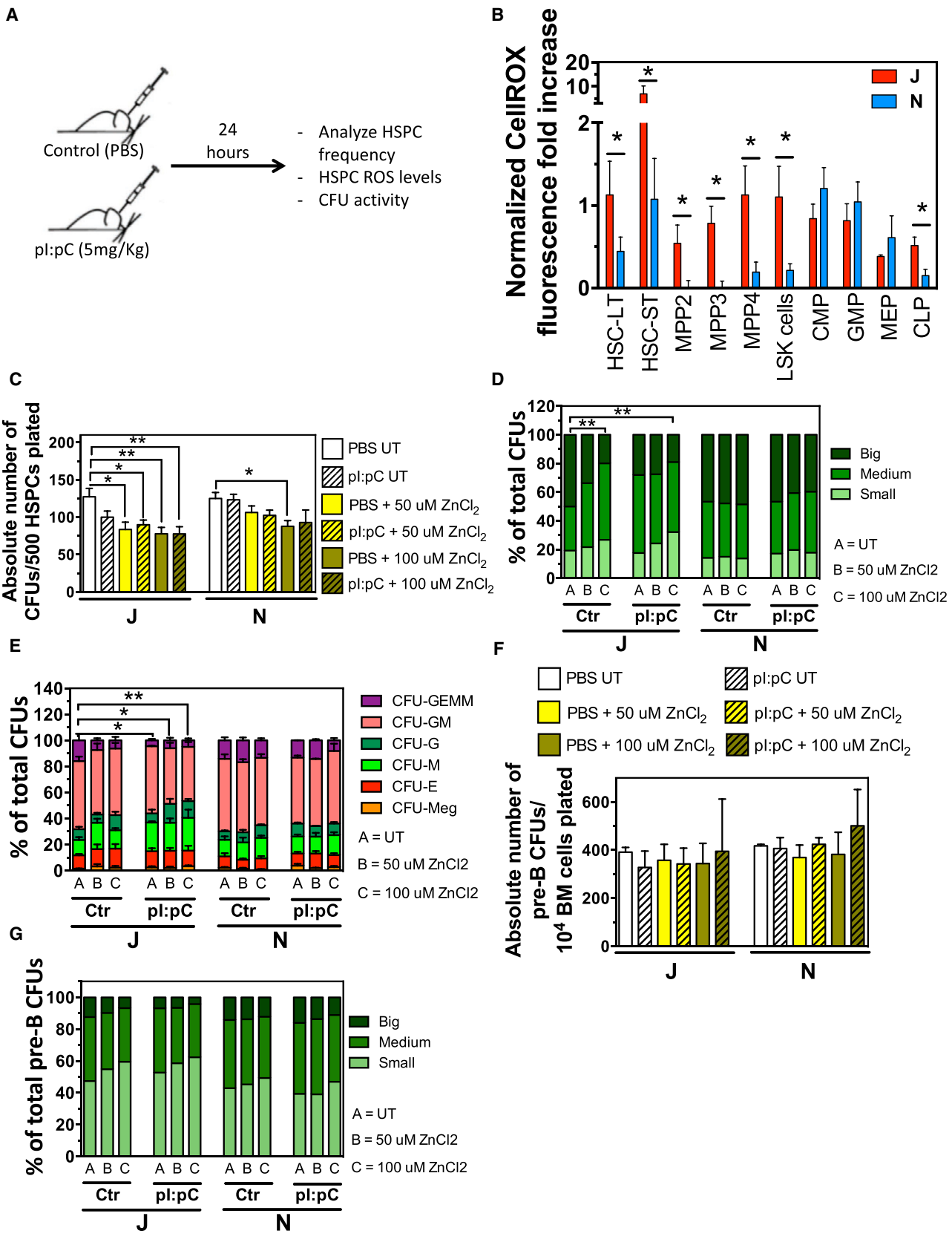

(legend on next page)

to a compromised ability to respond to elevated oxidative stress during transplantation relative to N-HSPCs. This deficiency was most apparent in lymphoid cells and their upstream progenitors. Although higher *Nnt* expression levels in MPPs compared with HSCs could explain the heightened sensitivity of MPP3s and MPP4s to *Nnt* loss, further studies are needed to clarify this point. LT-HSCs are the most multi-potent and have the highest self-renewal potential among the HSPC subsets (Pietras et al., 2015). In addition, LT-HSCs contribute to maintaining the hematopoietic system throughout life (Nakamura-Ishizu et al., 2014; Sawai et al., 2016). Altogether this makes them key players in the hematopoietic hierarchy. Thus, it is possible that LT-HSCs have developed redundant mechanisms to manage excessive ROS during hematopoietic stress, which could otherwise compromise their survival. On the other hand, MPP3 and MPP4 turn over more rapidly and are more restricted in their lineage potential. For this reason, they may not have developed the same repertoire of redundant mechanisms. Interestingly, the lymphoid potential of these progenitors appears to be most sensitive to compromised regulation of ROS levels. Emerging evidence reveals that the differentiation state of lymphocytes largely determines their fate in terms of function and persistence. Although several studies describe the functional consequences of oxygen radical-related immune-regulation, relatively little is known about the sensitivity of individual lymphocyte subsets and progenitors to oxidative stress (Kesarwani et al., 2013). For example, ROS are thought to have effects on T cell function and proliferation (Kesarwani et al., 2013). Low concentrations of ROS in T cells are a prerequisite for cell survival, while increased ROS accumulation can lead to apoptosis/necrosis (Kesarwani et al., 2013). In Ts65Dn mice, a model for Down syndrome, there is a decrease in CLPs due to higher levels of oxidative stress associated with a reduction of interleukin-7R (Lorenzo et al., 2011), which plays an essential role in lymphoid development and homeostasis by promoting proliferation and inhibiting apoptosis (Fry and Mackall, 2005; Mazzucchelli and Durum, 2007).

Many studies that use C57BL/6 mice fail to specify their precise genetic background (Fontaine and Davis, 2016). Only 36 of 197 papers with the term "hematopoietic progenitors" in the title and the term "C57BL" in any other field indicated the specific C57BL/6 substrain employed in their study. This is concerning given that multiple vendors distribute genetic mouse models in different C57BL/6 substrains. Indeed, there are C57BL/6J substrains that do not have the mutation in *Nnt* found in other J substrains and therefore are not suitable controls for the C57BL/6J animals distributed by the Jackson Laboratory (Fontaine and Davis, 2016). The International Knockout Mouse Consortium generates targeted embryonic stem cells and knockout mice in the N substrain, while many Cre-recombinase lines are in J mice (Fontaine and Davis, 2016). Therefore, careful attention to background substrain and/or backcrossing is necessary to avoid these confounding variables (Fontaine and Davis, 2016). Given our evidence that C57BL/6J and C57BL/6N HSPCs are not functionally equivalent, investigators should be cautious and be aware of the genetic background of any mouse model used in studies focused on oxidative stress and mitochondrial function in hematopoiesis; as well as those studies involving short-term reconstitution of the hematopoietic system and the contribution of specific HSPC populations to this process.

EXPERIMENTAL PROCEDURES

Mice

C57BL/6J mice and competitor mice (B6.SJL) were purchased from the Jackson Laboratory (Bar Harbor, ME), C57BL/6NCrl mice were obtained from the Charles Rivers Laboratory (Wilmington, MA). Recipient mice (CD45.1/CD45.2) were obtained by crossing C57BL/6J CD45.1 and C57BL/6J CD45.2 from the Jackson Laboratory. Mice were housed in our facilities for at least 3 weeks before each experiment. For all experiments, mice were 6–10 weeks old. All animal experiments were carried out according to procedures approved by the St. Jude Children's Research Hospital Institutional Animal Care and Use Committee, and all animals were housed in a pathogen-free facility.

Flow-Cytometry Analysis of Peripheral Blood and Bone Marrow

PB was collected from the retro-orbital sinus as previously described (Holmfeldt et al., 2016). PB chimerism and lineages post transplant were analyzed using an LSR Fortessa (BD Biosciences, San Jose, CA) after staining with anti-GR1 PerCP Cy5.5 (RB6-8C5) (eBiosciences #15-5931-83), anti-B220 PerCP Cy5.5

Figure 6. J-HSPCs Are Hypersensitive to Oxidative Stress Induction Relative to N-HSPCs

(A) Experimental schematic. BMC ROS levels and CFU potential were examined in J and N mice 24 hr after treatment with pI:pC.

(B) CellROX Deep Red fluorescence was measured in BMC from N and J control mice and after pI:pC injection. Fluorescence was normalized to the values of J control cells, and the increase of fluorescence between control and pI:pC injected mice was calculated.

(C–E) Number (C), size (D), and distribution (E) of CFUs generated by HSPCs from N and J control mice and after pI:pC injection.

(F and G) Number (F) and size (G) of pre-B colonies generated by HSPCs from N and J control mice and after pI:pC injection. $ZnCl_2$ was added to CFU and pre-B colonies assays to increase the production of ROS.

Data are presented as mean ± SEM, $n \geq 3$. *$p < 0.05$, **$p < 0.005$.

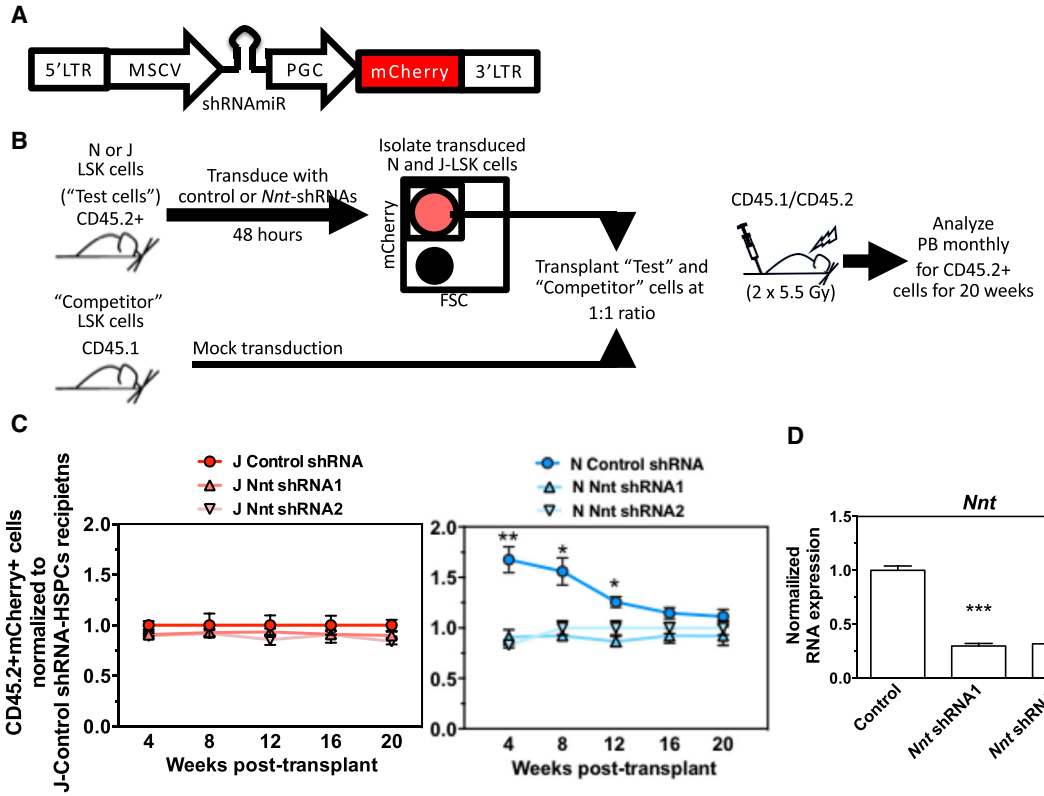

Figure 7. *Nnt* Knockdown in N-HSPCs Recapitulates J-HSPC Short-Term Repopulating Defect

(A) miR30-embedded shRNAs targeting *Nnt* were cloned into a lentiviral vector downstream of the MSCV promoter. The phosphoglycerate kinase (PGK) promoter drives mCherry.

(B) LSK cells isolated from N or J mice ($CD45.2^+$) were transduced with lentivirus containing control or *Nnt*-shRNAs. Transduced cells (i.e., $mCherry^+$) were then isolated and transplanted with an equal number of competitor LSK cells ($CD45.1^+$) into lethally irradiated recipients ($CD45.1/CD45.2^+$). Recipient PB was monitored by flow cytometry every 4 weeks for 20 weeks post transplant for $CD45.2^+$ $mCherry^+$ cells.

(C) Normalized percentage of $CD45.2^+$ $mCherry^+$ cells in the recipient mice PB after transplant. Data normalized to the $CD45.2^+$ $mCherry^+$ chimerism observed in recipients of J-LSK cells transduced with control shRNA.

(D) *Nnt* normalized gene expression in N-LSK cells transduced with control or *Nnt*-shRNAs.

Data from two independent transplants are presented as mean ± SEM. Donor mice, n = 3 per transplant. Recipient mice, n = 5 per transplant. *p < 0.05, **p < 0.005, ***p < 0.001, significantly different from recipients of J-LSK cells transduced with control shRNA.

(RA3-6B2) (Biolegend #103235), anti-CD11B PerCP Cy5.5 (M1/70) (Biolegend #101228), anti-B220 PE Cy7 (RA3-6B2) (Tonbo Biosciences #60-0452-U100), anti-CD4 PE Cy7 (RM4-5) (Tonbo Biosciences #60-0042-U025), anti-CD8 PE Cy7 (53-6.7) (Tonbo Biosciences #60-0081-U100), anti-CD45.1 FITC (104) (Biolegend #110706), and anti-CD45.2 V500 (A20) (BD #562129) (all at 1:200 dilution). DAPI (Sigma-Aldrich, St. Louis, MO) was used for dead cell exclusion.

BM was extracted from mice tibias, femurs, and pelvic bones. Bones were crushed and incubated in red blood cell lysis buffer (Sigma-Aldrich) for 5 min on ice. BMCs were visualized by flow cytometry after staining with the following antibodies: HSC-LT/HSC-ST/MPP2/MPP3/MPP4 (B220-PerCP [RA3-6B2] [Biolegend #553093], CD3-PerCP [145-2C11] [Biolegend #100326], CD4-PerCP [GK1.5] [Biolegend #100432], CD8-PerCP [53-6.7] [Biolegend #100732], CD19-PerCP [6D5] [Biolegend #115532], GR1-PerCP [RB6-8C5] [Biolegend #108426], TER119-PerCP [TER-119] [Biolegend #116226], SCA1-PerCP-Cy5.5 [E13-161.7] [Biolegend #122524], CKIT-APC-780 [2B8] [eBiosciences #47-1171-82], CD150-PE-Cy7 [TC15-12F12.2] [Biolegend #115914], CD48-Alexa Fluor 700 [HM48-1] [Biolegend #103426], FLT3-PE [A2F10.1] [BD #553842], CD45.1-FITC [104] [Biolegend #110706], and CD45.2-v500 [A20] [BD #562129]); CMP/GMP/MEP (B220-PerCP [RA3-6B2], CD3-PerCP [145-2C11], CD4-PerCP [GK1.5], CD8-PerCP [53-6.7], CD19-PerCP [6D5], GR1-PerCP [RB6-8C5], TER119-PerCP [TER-119], SCA1-PerCP-Cy5.5 [E13-161.7], CKIT-APC-780 [2B8], FCR II/III-Alexa Fluor 700 [93] [Biolegend #101317], CD34-FITC [RAM34] [BD #553733], CD45.1-FITC [104], and CD45.2-v500 [A20]); and CLP (B220-PerCP [RA3-6B2], CD3-PerCP [145-2C11], CD4-PerCP [GK1.5], CD8-PerCP [53-6.7], CD19-PerCP [6D5], GR1-PerCP [RB6-8C5], TER119-PerCP [TER-119], SCA1-PerCP-Cy5.5 [E13-161.7], CKIT-APC-780 [2B8], IL-7R-PE-Cy7 [A7R34] [Tonbo Biosciences #60-1271-U100], CD45.1-FITC [104], and CD45.2-v500 [A20]) (all at 1:200; except CD34 at 1:50).

Populations were identified according to the gating strategy described in Figure S6. DAPI (Sigma-Aldrich) was used for dead cell exclusion.

For PB and BM, data analysis was performed with FlowJo version 10 (LLC, Ashland, OR).

LSK (Lineage-SCA1$^+$CKIT$^+$) Cell Preparation

BM was extracted from femur, pelvic bone, and tibias via crushing. CKIT$^+$ cells were isolated via magnetic enrichment using anti-CD117 microbeads (Miltenyi Biotec, Carlsbad, CA) and an autoMACs magnetic cell separator (Miltenyi Biotec). Cells were then stained with anti-SCA1 PerCPCy5.5 (E13-161.7) and anti-CKIT APCe780 (2B8) to facilitate isolation of LSK cells by cell sorting on FACSAria III (BD Biosciences).

LSK Cell Transplantation

LSK cells from N and J mice were transplanted into CD45.1/CD45.2 recipient mice pre-irradiated with 11 Gy (two doses of 5.5 Gy separated by 3 hr). A 150-μL solution of PBS containing 5,000 test (J or N) LSK cells (CD45.2) and 5,000 competitor LSK cells (CD45.1) was injected into each recipient mouse via tail vein. Recipient mice received antibiotics (enrofloxacin, 1 mL/9.1 kg) in their water for 10 days post transplant. The frequency of CD45.2- and CD45.1-positive PB cells was assessed by flow cytometry every 4 weeks post transplant for at least 20 weeks. To minimize biological variation, for each transplant we collected and pooled femur, tibia, and hip bones from three individuals for collection of BM via crushing.

Secondary Transplantation

BM cells from N- and J-LSK cells primary recipient mice were transplanted into CD45.1/CD45.2 recipient mice pre-irradiated with 11 Gy (two doses of 5.5 Gy separated by 3 hr). A 150-μL solution of PBS containing 10^6 test (J or N) BM cells (CD45.2) was injected into each recipient mouse via tail vein. Recipient mice received antibiotics (enrofloxacin, 1 mL/9.1 kg) in their water for 10 days post transplant. The frequency of CD45.2- and CD45.1-positive PB cells was assessed by flow cytometry every 4 weeks post transplant for at least 20 weeks. To minimize biological variation, for each transplant we collected and pooled femur, tibia, and hip bones from five individuals for collection of BM via crushing.

Limiting Dilution Transplants

J- or N-BM cells (15,000, 30,000, 50,000 or 100,000 CD45.2$^+$) were injected with 2 × 10^5 CD45.1$^+$ WBM cells into lethally irradiated CD45.1$^+$/CD45.2$^+$ recipients. Engraftment was defined as >1% CD45.2 chimerism in the T cell, B cell, and myeloid lineages of recipient PB after transplant. l-Calc (STEMCELL Technologies, Vancouver, Canada) was used to analyze the results of the limiting dilution transplants.

HSPC Subsets Transplantation

HSPC subsets (LT-HSC, ST-HSC, MPP2, MPP3, and MPP4) from N and J mice were transplanted into CD45.1/CD45.2 recipient mice sublethally pre-irradiated with 9.5 Gy (two doses of 4.75 Gy separated by 3 hr). A 150-μL solution of PBS containing 2,000 cells of each subset (CD45.2) was injected into each recipient mouse via tail vein. Recipient mice received antibiotics (enrofloxacin, 1 mL/9.1 kg) in their water for 10 days post transplant. The frequency of CD45.2 PB cells was assessed by flow cytometry every 3–4 days post transplant for 34–100 days.

Colony-Forming Unit Assays

Five hundred LSK cells were plated in M3434 methylcellulose (STEMCELL). Colonies were scored 8–10 days later. For pre-B CFU assays, 1 × 10^5 BM cells were plated in M3630 methylcellulose (STEMCELL). Colonies were then scored 7 days later.

Oxidative Stress Induction Experiments

To provoke increased ROS in HSPCs, we injected 5 mg/kg of pI:pC intraperitoneally into J and N mice. Control J and N mice were injected with the same volume of PBS. Twenty-four hours later, BM was isolated from control and treated mice, and the BMC frequency and their ROS levels were analyzed by CellROX Deep Red (Thermo Fisher Scientific, Waltham, MA) staining and flow cytometry. Five hundred LSK cells were plated in M3434 methylcellulose (STEMCELL). Colonies were scored 8–10 days later. For pre-B CFU assays, 1 × 10^5 BM cells were plated in M3630 methylcellulose (STEMCELL). Different concentrations of $ZnCl_2$ were added to the methylcellulose to induce a further increase in ROS levels. Colonies were then scored 7 days later.

shRNAs

shRNAs were designed as previously described (Fellmann et al., 2011; Holmfeldt et al., 2013). Gene knockdown (KD) efficiency in LSK cells was quantified by qRT-PCR after normalizing to transduction frequency (Figure 7D).

Nnt *shRNA1*

TGC TGT TGA CAG TGA GCG GGA GGA TAC GCG AAA GAG ATG TTA GTG AAG CCA CAG ATG TAA CAT CTC TTT CGC GTA TCC TCC TGC CTA CTG CCT CGG A.

Nnt *shRNA2*

TGC TGT TGA CAG TGA GCG GCT ATA ACA TCG AAG AAA TCA TTA GTG AAG CCA CAG ATG TAA TGA TTT CTT CGA TGT TAT AGC TGC CTA CTG CCT CGG A.

Lentiviral Production

Vesicular stomatitis virus glycoprotein-pseudotyped lentivirus was prepared as previously described using a four-plasmid system (Transfer vector, Gag/Pol, Rev/Tat, and vesicular stomatitis virus glycoprotein envelope plasmid) by co-transfection of 293T cells using TransIT 293 (Mirus) (Holmfeldt et al., 2013). Viral supernatant was collected 48 hr later, cleared, and stored at −80°C. Viral preparations were titered on 293T cells.

LSK Cell Culture and Transduction

LSK cells were isolated from 6- to 10-week-old murine BM and transduced with lentivirus as previously described (Holmfeldt et al., 2013). In brief, non-tissue culture 96-well plates were coated with Retronectin (TaKaRa Bio, Shiga, Japan) according to the manufacturer's instructions. Lentiviral particles corresponding to an MOI of 25 were spin loaded onto the plates for 1 hr at 1,000 × *g*

at room temperature. Wells were washed with PBS, followed by the addition of 15,000 freshly isolated LSK cells resuspended in 200 μL of serum-free expansion medium (STEMCELL) with 10 ng/mL recombinant murine (RM) stem cell factor, 20 ng/mL RM thrombopoietin, 20 ng/mL RM insulin-like growth factor 2 (PeproTech, Rocky Hill, NJ), 10 ng/mL recombinant human fibroblast growth factor 1 (R&D Systems, Minneapolis, MN), and 5 μg/mL protamine sulfate (Sigma-Aldrich). Cells were incubated at 37°C. For collection of cells for transplantation 48 hr after transduction, medium was slowly removed and cells were washed and resuspended in PBS 1.5% fetal calf serum.

Nnt *Expression Quantification*

HSPCs subsets (LT-HSC, ST-HSC, MPP2, MPP3, and MPP4) were isolated from N mice and *Nnt* expression was analyzed by qRT-PCR with the following primers:

Fw *Nnt*: TCC AAA ACG AGA AGC GAG TT.

Rv *Nnt*: TCC TTC ATC CCT TGG ATC TG.

Statistical Analysis

Statistical significance for comparisons between two groups was assessed using two-sample t tests or exact Wilcoxon Mann-Whitney tests, depending on the normality test based on the Shapiro-Wilk test. Tests were performed using GraphPad Prism 4.0 software (GraphPad, San Diego, CA).

SUPPLEMENTAL INFORMATION

Supplemental Information includes six figures and can be found with this article online at https://doi.org/10.1016/j.stemcr.2018.06.011.

AUTHOR CONTRIBUTIONS

A.M.H. and S.M.-F. wrote, reviewed, and revised the manuscript and designed the experiments. A.M.H., A.M., and A.C. performed the experiments. G.K. performed the statistical analysis.

ACKNOWLEDGMENTS

We thank Trent Hall, Megan Walker, Margaret Goodell, the McKinney-Freeman laboratory, and the Clements laboratory for critical discussions and reading of the manuscript; D. Ashmun, D. Langfitt, L. He, S. Schwemberger, and S. Wollard for FACS support; and A. Reap, C. Davis-Goodrum, and K. Millican for help with mouse injections. This work was supported by the American Lebanese Syrian Associated Charities (ALSAC) (S.M.-F.) and the National Institute for Diabetes and Digestive and Kidney Diseases at the NIH (R01 DK104028, S.M.-F.).

Received: September 21, 2017
Revised: June 13, 2018
Accepted: June 14, 2018
Published: July 12, 2018

REFERENCES

Cao, Y., Fang, Y., Cai, J., Li, X., Xu, F., Yuan, N., Zhang, S., and Wang, J. (2016). ROS functions as an upstream trigger for autophagy to drive hematopoietic stem cell differentiation. Hematology *21*, 613–618.

Chen, C., Liu, Y., Liu, R., Ikenoue, T., Guan, K.L., Liu, Y., and Zheng, P. (2008). TSC-mTOR maintains quiescence and function of hematopoietic stem cells by repressing mitochondrial biogenesis and reactive oxygen species. J. Exp. Med. *205*, 2397–2408.

Chen, C., Liu, Y., Liu, Y., and Zheng, P. (2009). The axis of mTOR-mitochondria-ROS and stemness of the hematopoietic stem cells. Cell Cycle *8*, 1158–1160.

Clapcote, S.J., and Roder, J.C. (2004). Survey of embryonic stem cell line source strains in the water maze reveals superior reversal learning of 129S6/SvEvTac mice. Behav. Brain Res. *152*, 35–48.

Diwan, B.A., and Blackman, K.E. (1980). Differential susceptibility of 3 sublines of C57BL6 mice to the induction of colorectal tumors by 1,2-dimethylhydrazine. Cancer Lett. *9*, 111–115.

Ergen, A.V., and Goodell, M.A. (2010). Mechanisms of hematopoietic stem cell aging. Exp. Gerontol. *45*, 286–290.

Fellmann, C., Zuber, J., McJunkin, K., Chang, K., Malone, C.D., Dickins, R.A., Xu, Q., Hengartner, M.O., Elledge, S.J., Hannon, G.J., et al. (2011). Functional identification of optimized RNAi triggers using a massively parallel sensor assay. Mol. Cell *41*, 733–746.

Fontaine, D.A., and Davis, D.B. (2016). Attention to background strain is essential for metabolic research: C57BL/6 and the international knockout mouse consortium. Diabetes *65*, 25–33.

Freeman, H.C., Hugill, A., Dear, N.T., Ashcroft, F.M., and Cox, R.D. (2006). Deletion of nicotinamide nucleotide transhydrogenase: a new quantitative trait locus accounting for glucose intolerance in C57BL/6J mice. Diabetes *55*, 2153–2156.

Fry, T.J., and Mackall, C.L. (2005). The many faces of IL-7: from lymphopoiesis to peripheral T cell maintenance. J. Immunol. *174*, 6571–6576.

Green, M.L., Singh, A.V., Zhang, Y., Nemeth, K.A., Sulik, K.K., and Knudsen, T.B. (2007). Reprogramming of genetic networks during initiation of the fetal alcohol syndrome. Dev. Dyn. *236*, 613–631.

Grottick, A.J., Bagnol, D., Phillips, S., McDonald, J., Behan, D.P., Chalmers, D.T., and Hakak, Y. (2005). Neurotransmission- and cellular stress-related gene expression associated with prepulse inhibition in mice. Brain Res. Mol. Brain Res. *139*, 153–162.

Hao, Y., Cheng, D., Ma, Y., Zhou, W., and Wang, Y. (2011). Antioxidant intervention: a new method for improving hematopoietic reconstitution capacity of peripheral blood stem cells. Med. Hypotheses *76*, 421–423.

Hoek, J.B., and Rydström, J. (1988). Physiological roles of nicotinamide nucleotide transhydrogenase. Biochem. J. *254*, 1–10.

Holmfeldt, P., Ganuza, M., Marathe, H., He, B., Hall, T., Kang, G., Moen, J., Pardieck, J., Saulsberry, A.C., Cico, A., et al. (2016). Functional screen identifies regulators of murine hematopoietic stem cell repopulation. J. Exp. Med. *213*, 433–449.

Holmfeldt, P., Pardieck, J., Saulsberry, A.C., Nandakumar, S.K., Finkelstein, D., Gray, J.T., Persons, D.A., and McKinney-Freeman, S. (2013). Nfix is a novel regulator of murine hematopoietic stem and progenitor cell survival. Blood *122*, 2987–2996.

Huang, T.T., Naeemuddin, M., Elchuri, S., Yamaguchi, M., Kozy, H.M., Carlson, E.J., and Epstein, C.J. (2006). Genetic modifiers of

the phenotype of mice deficient in mitochondrial superoxide dismutase. Hum. Mol. Genet. *15*, 1187–1194.

Huang, Y.C., Hwang, T.L., Yang, Y.L., Wu, S.H., Hsu, M.H., Wang, J.P., Chen, S.C., Huang, L.J., and Liaw, C.C. (2010). Acetogenin and prenylated flavonoids from Helminthostachys zeylanica with inhibitory activity on superoxide generation and elastase release by neutrophils. Planta Med. *76*, 447–453.

Ito, K., Hirao, A., Arai, F., Matsuoka, S., Takubo, K., Hamaguchi, I., Nomiyama, K., Hosokawa, K., Sakurada, K., Nakagata, N., et al. (2004). Regulation of oxidative stress by ATM is required for self-renewal of haematopoietic stem cells. Nature *431*, 997–1002.

Ito, K., Hirao, A., Arai, F., Takubo, K., Matsuoka, S., Miyamoto, K., Ohmura, M., Naka, K., Hosokawa, K., Ikeda, Y., et al. (2006). Reactive oxygen species act through p38 MAPK to limit the lifespan of hematopoietic stem cells. Nat. Med. *12*, 446–451.

Kesarwani, P., Murali, A.K., Al-Khami, A.A., and Mehrotra, S. (2013). Redox regulation of T-cell function: from molecular mechanisms to significance in human health and disease. Antioxid. Redox Signal. *18*, 1497–1534.

Khisti, R.T., Wolstenholme, J., Shelton, K.L., and Miles, M.F. (2006). Characterization of the ethanol-deprivation effect in substrains of C57BL/6 mice. Alcohol *40*, 119–126.

Kinazaki, A., Chen, H., Koizumi, K., Kawanai, T., Oyama, T.M., Satoh, M., Ishida, S., Okano, Y., and Oyama, Y. (2011). Putative role of intracellular $Zn(2^{+})$ release during oxidative stress: a trigger to restore cellular thiol content that is decreased by oxidative stress. J. Physiol. Sci. *61*, 403–409.

Le, Q., Yao, W., Chen, Y., Yan, B., Liu, C., Yuan, M., Zhou, Y., and Ma, L. (2016). GRK6 regulates ROS response and maintains hematopoietic stem cell self-renewal. Cell Death Dis. *7*, e2478.

Lewandowski, D., Barroca, V., Duconge, F., Bayer, J., Van Nhieu, J.T., Pestourie, C., Fouchet, P., Tavitian, B., and Romeo, P.H. (2010). In vivo cellular imaging pinpoints the role of reactive oxygen species in the early steps of adult hematopoietic reconstitution. Blood *115*, 443–452.

Lin, C.C., Lee, I.T., Wu, W.L., Lin, W.N., and Yang, C.M. (2012). Adenosine triphosphate regulates NADPH oxidase activity leading to hydrogen peroxide production and COX-2/PGE2 expression in A549 cells. Am. J. Physiol. Lung Cell Mol. Physiol. *303*, L401–L412.

Lorenzo, L.P., Chen, H., Shatynski, K.E., Clark, S., Yuan, R., Harrison, D.E., Yarowsky, P.J., and Williams, M.S. (2011). Defective hematopoietic stem cell and lymphoid progenitor development in the Ts65Dn mouse model of Down syndrome: potential role of oxidative stress. Antioxid. Redox Signal. *15*, 2083–2094.

Mantel, C.R., O'Leary, H.A., Chitteti, B.R., Huang, X., Cooper, S., Hangoc, G., Brustovetsky, N., Srour, E.F., Lee, M.R., Messina-Graham, S., et al. (2015). Enhancing hematopoietic stem cell transplantation efficacy by mitigating oxygen shock. Cell *161*, 1553–1565.

Maryanovich, M., Zaltsman, Y., Ruggiero, A., Goldman, A., Shachnai, L., Zaidman, S.L., Porat, Z., Golan, K., Lapidot, T., and Gross, A. (2015). An MTCH2 pathway repressing mitochondria metabolism regulates haematopoietic stem cell fate. Nat. Commun. *6*, 7901.

Mayorga, A.J., and Lucki, I. (2001). Limitations on the use of the C57BL/6 mouse in the tail suspension test. Psychopharmacology *155*, 110–112.

Mazzucchelli, R., and Durum, S.K. (2007). Interleukin-7 receptor expression: intelligent design. Nat. Rev. Immunol. *7*, 144–154.

Mekada, K., Abe, K., Murakami, A., Nakamura, S., Nakata, H., Moriwaki, K., Obata, Y., and Yoshiki, A. (2009). Genetic differences among C57BL/6 substrains. Exp. Anim. *58*, 141–149.

Nakamura-Ishizu, A., Takizawa, H., and Suda, T. (2014). The analysis, roles and regulation of quiescence in hematopoietic stem cells. Development *141*, 4656–4666.

Pietras, E.M., Reynaud, D., Kang, Y.A., Carlin, D., Calero-Nieto, F.J., Leavitt, A.D., Stuart, J.M., Gottgens, B., and Passegue, E. (2015). Functionally distinct subsets of lineage-biased multipotent progenitors control blood production in normal and regenerative conditions. Cell Stem Cell *17*, 35–46.

Radulovic, J., Kammermeier, J., and Spiess, J. (1998). Generalization of fear responses in C57BL/6N mice subjected to one-trial foreground contextual fear conditioning. Behav. Brain Res. *95*, 179–189.

Ronchi, J.A., Figueira, T.R., Ravagnani, F.G., Oliveira, H.C., Vercesi, A.E., and Castilho, R.F. (2013). A spontaneous mutation in the nicotinamide nucleotide transhydrogenase gene of C57BL/6J mice results in mitochondrial redox abnormalities. Free Radic. Biol. Med. *63*, 446–456.

Roth, D.M., Swaney, J.S., Dalton, N.D., Gilpin, E.A., and Ross, J., Jr. (2002). Impact of anesthesia on cardiac function during echocardiography in mice. Am. J. Physiol. Heart Circ. Physiol. *282*, H2134–H2140.

Sawai, C.M., Babovic, S., Upadhaya, S., Knapp, D.J.H.F., Lavin, Y., Lau, C.M., Goloborodko, A., Feng, J., Fujisaki, J., Ding, L., et al. (2016). Hematopoietic stem cells are the major source of multilineage hematopoiesis in adult animals. Immunity *45*, 597–609.

Siegmund, A., Langnaese, K., and Wotjak, C.T. (2005). Differences in extinction of conditioned fear in C57BL/6 substrains are unrelated to expression of alpha-synuclein. Behav. Brain Res. *157*, 291–298.

Simon, M.M., Greenaway, S., White, J.K., Fuchs, H., Gailus-Durner, V., Wells, S., Sorg, T., Wong, K., Bedu, E., Cartwright, E.J., et al. (2013). A comparative phenotypic and genomic analysis of C57BL/6J and C57BL/6N mouse strains. Genome Biol. *14*, R82.

Stiedl, O.R., Radulovic, J., Lohmann, R., Birkenfeld, K., Palve, M., Kammermeier, J., Sananbenesi, F., and Spiess, J. (1999). Strain and substrain differences in context- and tone-dependent fear conditioning of inbred mice. Behav. Brain Res. *104*, 1–12.

Strohecker, A.M., Joshi, S., Possemato, R., Abraham, R.T., Sabatini, D.M., and White, E. (2015). Identification of 6-phosphofructo-2-kinase/fructose-2,6-bisphosphatase as a novel autophagy regulator by high content shRNA screening. Oncogene *34*, 5662–5676.

Testa, U., Labbaye, C., Castelli, G., and Pelosi, E. (2016). Oxidative stress and hypoxia in normal and leukemic stem cells. Exp. Hematol. *44*, 540–560.

Toye, A.A., Lippiat, J.D., Proks, P., Shimomura, K., Bentley, L., Hugill, A., Mijat, V., Goldsworthy, M., Moir, L., Haynes, A., et al.

(2005). A genetic and physiological study of impaired glucose homeostasis control in C57BL/6J mice. Diabetologia *48*, 675–686.

Walter, D., Lier, A., Geiselhart, A., Thalheimer, F.B., Huntscha, S., Sobotta, M.C., Moehrle, B., Brocks, D., Bayindir, I., Kaschutnig, P., et al. (2015). Exit from dormancy provokes DNA-damage-induced attrition in haematopoietic stem cells. Nature *520*, 549–552.

Wiseman, D.A., Sharma, S., and Black, S.M. (2010). Elevated zinc induces endothelial apoptosis via disruption of glutathione metabolism: role of the ADP translocator. Biometals *23*, 19–30.

Yilmaz, O.H., Kiel, M.J., and Morrison, S.J. (2006). SLAM family markers are conserved among hematopoietic stem cells from old and reconstituted mice and markedly increase their purity. Blood *107*, 924–930.

Stem Cell Reports, Volume *11*

Supplemental Information

Elevated Oxidative Stress Impairs Hematopoietic Progenitor Function in C57BL/6 Substrains

Antonio Morales-Hernández, Alice Martinat, Ashley Chabot, Guolian Kang, and Shannon McKinney-Freeman

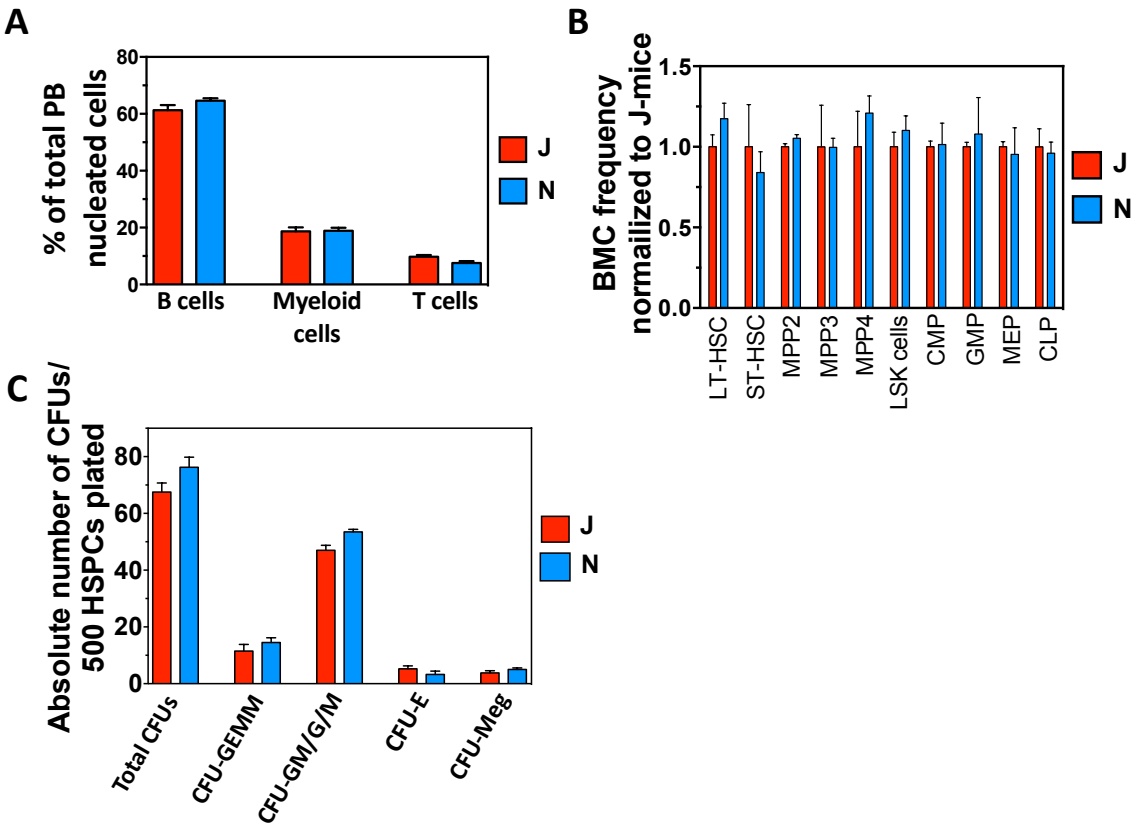

Figure S1. N and J-mice display a similar hematopoietic system under homeostatic conditions.
A. Percentage of myeloid (GR1+CD11B+) and lymphoid (B cells as B220+ and T cells as CD4+CD8+) lineage cells in the PB of N and J-mice. **B.** Absolute frequency of BMC (HSC-LT; HSC-ST; MPP; LSK cells; CMP; GMP; MEP; CLP) of N and J-mice. Data presented are normalized to the absolute levels in J-mice. **C.** LSK cells from N and J-mice were assayed for CFU potential. Data represented as mean ± SEM. ≥ 4 mice were examined in A-C.

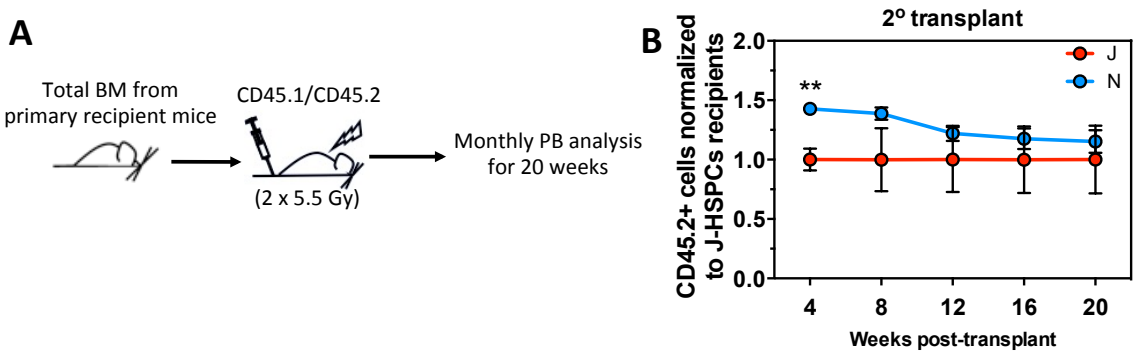

Figure S2. J-BM cells display short-term repopulating defect in secondary transplants. Related to Figure 1. A. 10^6 BM cells from primary transplant recipients were injected into lethally irradiated recipient mice (CD45.1/CD45.2). The PB of secondary recipients was examined every four weeks for 20 weeks post-transplant for CD45.2+ cells. **B.** Normalized CD45.2+ cells percentage in recipient mice PB after secondary transplant. Recipient mice CD45.2+ cells percentage was corrected to the original injected CD45.2+ cells percentage. Data presented are normalized to the CD45.2+ cells percentage observed in recipients of J-LSK cells. Data represented as mean ± SEM. Donor mice $N \geq 5$ per transplant. Recipient mice $N \geq 5$ per transplant. ** $p < 0.005$ significantly different to recipients of J-BM cells.

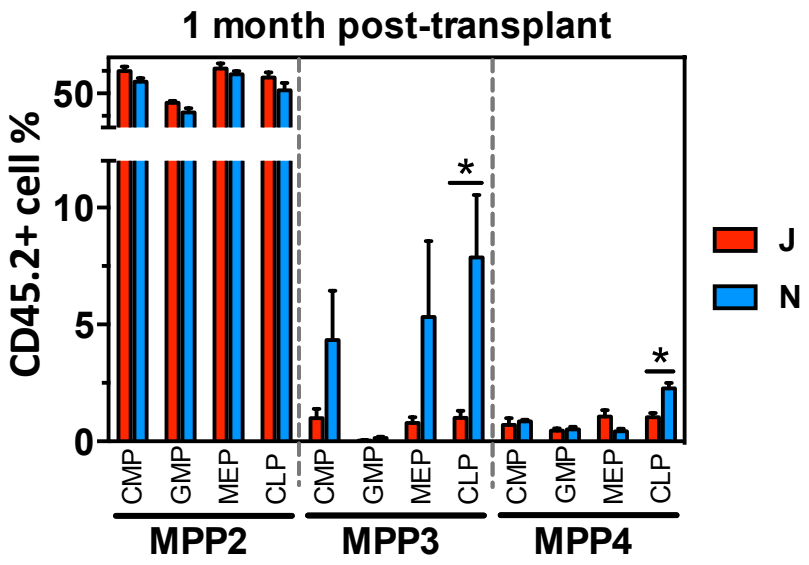

Figure S3. J-MMP3 and MPP4 cells display a CLP repopulating defect compared with N-MPP3 and MPP4 cells. Related to Figure 3. CD45.2+ MPP2, MPP3 or MPP4 cells from J or N mice were transplanted into sub-lethally irradiated recipients (CD45.1/CD45.2). Normalized CD45.2+ cells percentage of each BMC one month post-transplant. Data presented are normalized to the CD45.2+ cells percentage in J-mice. Data from two independent transplants represented as mean ± SEM. Donor mice $N \geq 3$ pooled per transplant. Recipient mice $N \geq 5$ per transplant. * $p < 0.05$ significantly different to recipients of J-HSPCs.

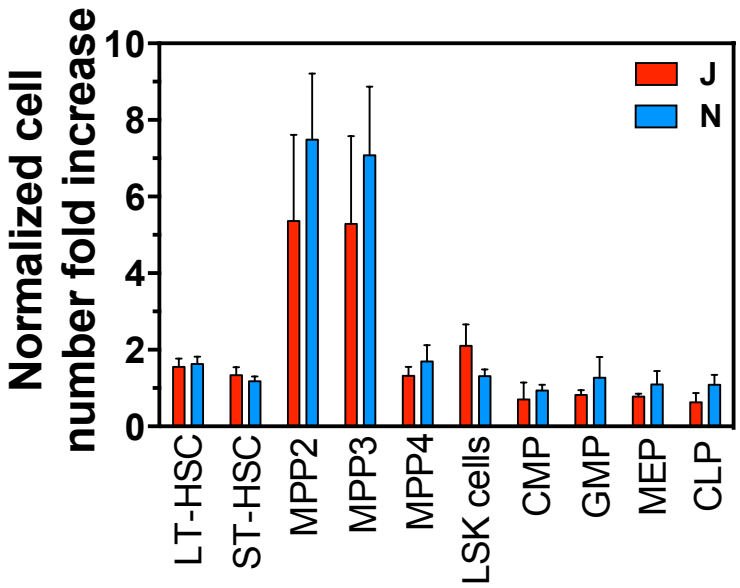

Figure S4. Similarly elevated BMC numbers in pI:pC treated J and N-mice. Related to Figure 6. 24 hours post-pI:pC injection, the absolute frequency of BMC (LT-HSC; ST-HSC; MPP; LSK cells; CMP; GMP; MEP; CLP) of N and J-mice was analyzed. The increase between control and pI:pC injected animals is shown. Data are presented as mean ±SEM. N = 3.

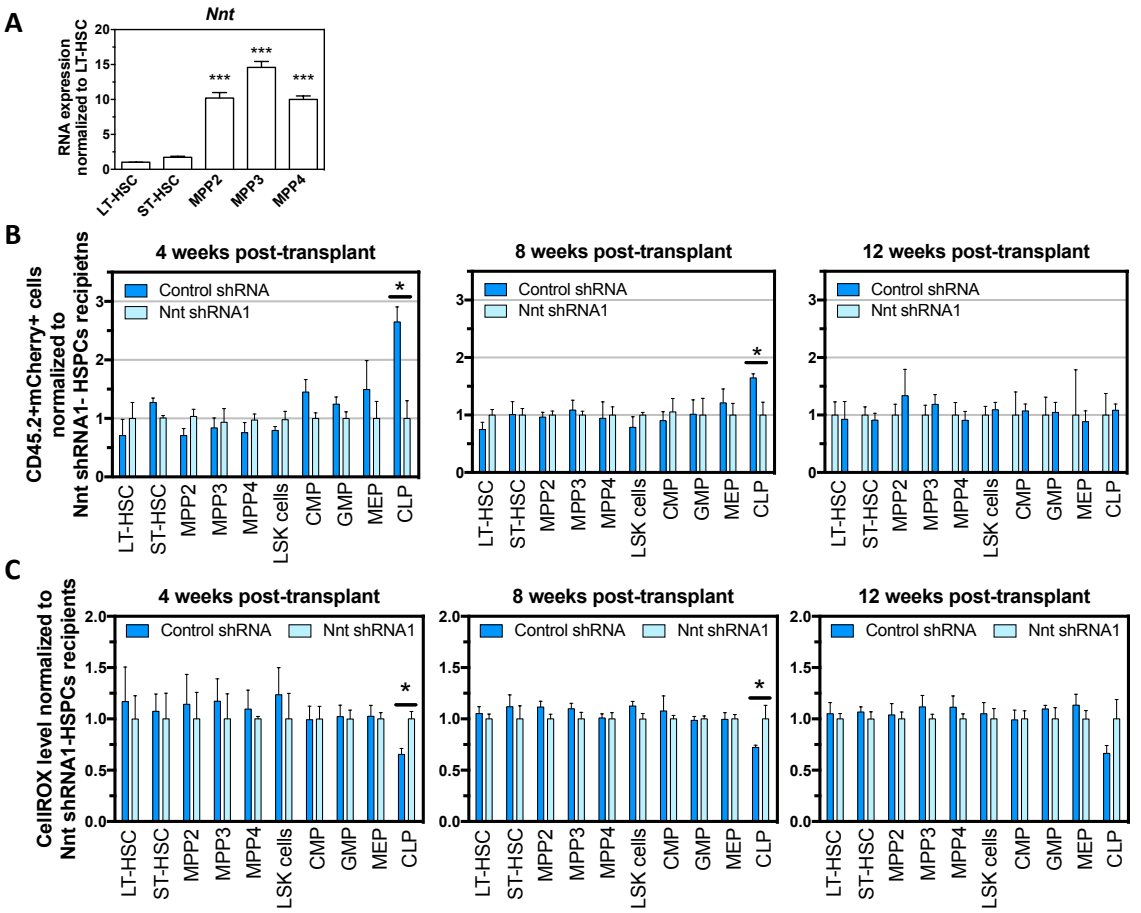

Figure S5. N-HSPCs express *Nnt* at different levels and *Nnt* knockdown in N-HSPCs recapitulates J-HSPC short-term repopulating defect. Related to Figure 7. A. LT-HSC, ST-HSC, MPP2, MPP3 and MPP4 were isolated from N-mice and *Nnt* expression was quantified by RT-qPCR. Data are presented as mean ±SEM. N = 2. *** $p < 0.001$ significantly different to LT-HSC. LSK cells isolated from N or J-mice (CD45.2+) were transduced with lentivirus containing control or *Nnt*-shRNAs. Transduced cells (i.e. mCherry+) were then isolated and transplanted with an equal number of competitor LSK cells (CD45.1+) into lethally irradiated recipients (CD45.2+/CD45.1+). The frequency (**B**) and ROS levels (**C**) of CD45.2+mCherry+ cells in the bone marrow of recipients was then analyzed by flow cytometry every four weeks for 12 weeks post-transplant. Data represented as mean ±SEM. Donor mice N = 3 per transplant. Recipient mice N = 5 per transplant. * $p < 0.05$ significantly different to recipients of N-LSK cells transduced with *Nnt*-shRNA.

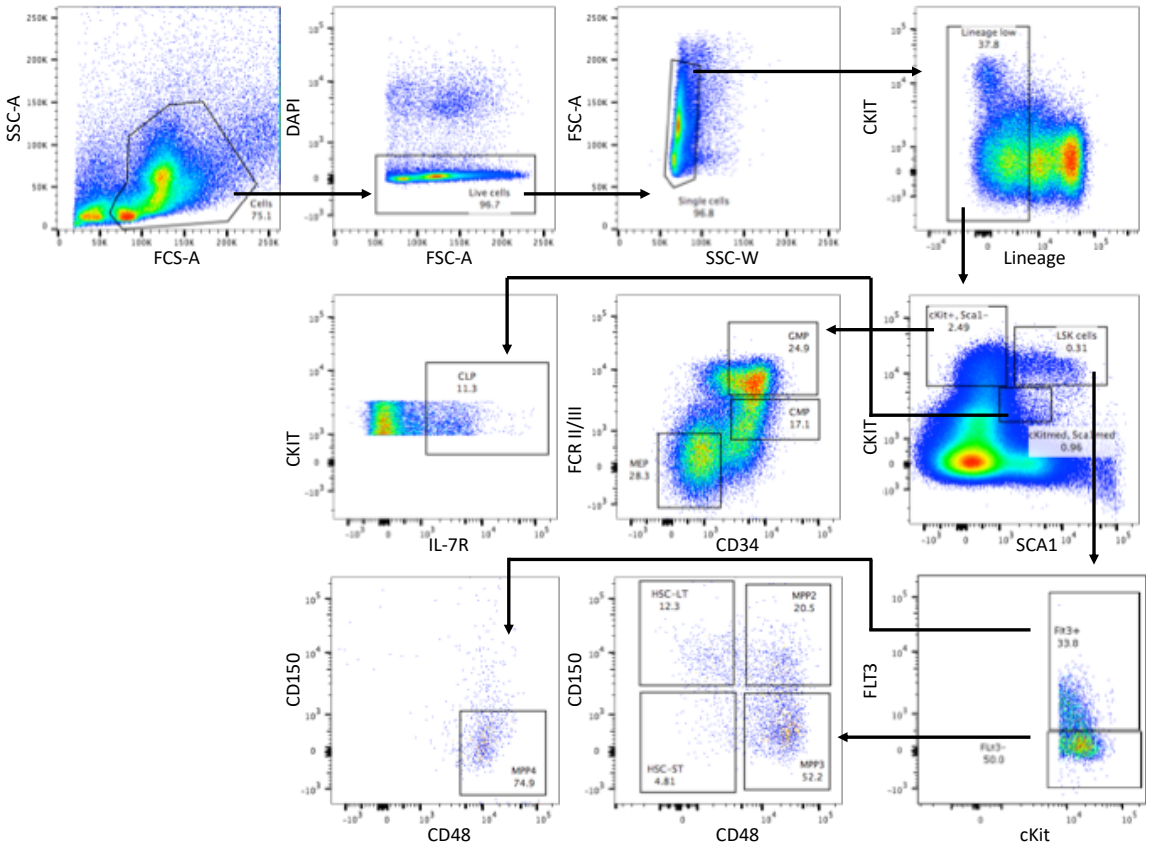

Figure S6. BMC gating strategy. Related to Figure 1-7, S1, S3, S4 and S5. Identification of each BMC according to their specific surface markers expression. LT-HSC (Lin$^-$SCA1$^+$CKIT$^+$FLT3$^-$CD150$^+$CD48$^-$); ST-HSC (Lin$^-$SCA1$^+$CKIT$^+$FLT3$^-$CD150$^-$CD48$^-$); MPP2 (Lin$^-$,Sca-1$^+$c-Kit$^+$Flt3$^-$CD150$^+$CD48$^+$); MPP3 (Lin$^-$SCA1$^+$CKIT $^+$FLT3$^-$CD150$^-$CD48$^+$); MPP4 (Lin$^-$SCA1$^+$CKIT $^+$FLT3$^-$CD150$^-$CD48$^+$); CMP (Lin$^-$SCA1$^-$ CKIT $^+$CD34$^+$FCR II/III^{med}); GMP (Lin$^-$SCA1$^-$CKIT$^+$CD34$^+$FCR II/III^{high}); MEP (Lin$^-$SCA1$^-$CKIT $^+$CD34$^-$FCR II/III$^-$); CLP (Lin$^-$SCA1^{med}CKIT^{med} IL-7R$^+$).